RNase H1 can catalyse RNA/DNA formation and cleavage with stable hairpin or duplex DNA oligomers

2 AUTHORS, INCLUDING:

Roger Wartell
Georgia Institute of Technology

90 PUBLICATIONS **2,744** CITATIONS

RNase H1 Can Catalyze RNA/DNA Hybrid Formation and Cleavage with Stable Hairpin or Duplex DNA Oligomers[†]

Jing Li and Roger M. Wartell*

School of Biology, Georgia Institute of Technology, Atlanta, Georgia 30332-0230

Received December 15, 1997; Revised Manuscript Received February 6, 1998

ABSTRACT: Cleavage of a RNA target site by RNase H1 from *Escherichia coli* was examined in the presence of complementary DNA sequences in the form of single-stranded, duplex, and hairpin structures. The target site was a 15 nt sequence in the middle of a 79 nt RNA transcript. DNA molecules employed included seven single-stranded oligodeoxynucleotides 10 or 15 nt long, and five hairpin DNAs each with a 10 bp stem and 5 nt loop. The loop and 3′ side of the stem of two of the hairpin DNAs were fully complementary to the target site, while the other hairpin DNAs had sequence changes. A 10 bp duplex DNA with one strand complementary to the target site was also employed. A gel electrophoresis mobility shift assay examined hybrid formation between the RNA and the single-stranded 15 nt DNA and two hairpin DNAs that contained 15 complementary bases. RNA titration of the ^{32}P-labeled single-stranded DNA produced a shifted band indicative of RNA/DNA complex formation. No RNA/DNA complex was detected when the more stable (T_m = 71 °C) hairpin DNA was combined with excess RNA. The less stable hairpin DNA (T_m = 62 °C) showed a small amount (∼8%) of hybrid formation. Thermodynamic analysis of RNA binding to the DNAs was in qualitative agreement with the results. Although no RNA/DNA hybrid was expected from thermodynamic calculations, a RNase H assay at 25 °C showed that hairpin or duplex DNAs with a 10 nt complementary sequence catalyzed RNA degradation. A complementary loop sequence in the hairpin DNA was not required. Cleavage of the RNA did not occur with hairpin DNAs containing three or four noncomplementary bases in the stem. The results show that RNase H can promote the formation and cleavage of a RNA/DNA hybrid between an RNA site and a base paired strand of a stable hairpin or duplex DNA at temperatures below their T_m.

Many cellular processes involve the formation of RNA/DNA hybrids. Examples occur in DNA replication initiation (*1−3*), DNA lagging strand synthesis (*4, 5*), RNA transcription (*6*), reverse transcription of RNA by retroviruses (*7*), recombination in immunoglobulin class switching (*8, 9*), and the maintenance of the eukaryotic chromosome telomeres by telomerase (*10, 11*). RNA/DNA hybrid formation is also the basis for the development of short antisense oligodeoxynucleotides for antiviral and antitumor therapy (*12*).

RNase H[1] is a ubiquitous enzyme found in both prokaryotic and eukaryotic cells (*13−16*), as well as in viruses (*17−19*). The enzyme binds to RNA/DNA duplexes and catalyzes the hydrolysis of the phosphodiester bond linkages in the RNA strand. The digestion of the RNA produces 5′-phosphate and 3′-hydroxy termini (*20, 21*). The three-dimensional structure of *E. coli* RNase H1 (*22*) has a region that appears to be the binding site for a RNA/DNA hybrid.

The widespread existence of RNase H implies it has an important role in biological processes. It is involved in DNA replication (*23, 24*) and in the reverse transcription of the retroviral RNA (*19*). RNase H was identified as a key factor

in the inhibition of gene expression induced by antisense oligonucleotides (*25, 26*). The minimum size of a RNA·DNA hybrid for cleavage by the enzyme is four base pairs (*27*). Although RNase H cleavage of RNA/DNA hybrids does not show sequence specificity, its effectiveness at cleaving a specific hybrid is expected to be influenced by the stability of competing RNA and DNA self-structures.

Thermodynamic studies have shown that the stability of a RNA/DNA hybrid vs homologous RNA and DNA duplexes depends on the identity of the bases in the RNA and DNA strands (*28−33*). In general, the order of thermal stability of nucleic acid base pairing is: RNA/RNA > r(purine)/d(pyrimidine) > DNA/DNA > r(pyrimidine)/d(purine). An exception occurs for duplexes with $(A)_n/(T/U)_n$ stretches which have the following order of thermal stability: dA/dT > rA/dT > rA/rU ≫ dA/rU (*34, 35*).

In this study, we examined the ability of RNase H to cleave a target site within a RNA when the complementary DNA sequence was presented as a single strand, a hairpin, or a duplex. The targeted 15 nt RNA segment is in the middle of a 79 nt RNA transcript. It is within a 30 nt sequence from the HIV-1 isolate MN that contains 10 consecutive pyrimidines (*36*). The sequence is in the reverse transcriptase gene of many different strains of HIV-1 by NCBI Blast Search. Results from gel shift experiments and thermodynamic analysis indicated that the RNA and a target-complementary hairpin DNA do not form a RNA/DNA

Table 1: Characteristics of Oligodeoxynucleotides (ODNs) Used in This Study[a]

ODNs	Sequence	T_m (°C)	% RNA degradation 25°C	% RNA degradation 37°C
H0A	5'-CCCGACGTTA**TT** |||**|*||| **C** 3'-**GGGAGGGAATCA**	60	71	79.4
H0B	5'-CCCTCCCTTA**TT** ||||||||| **C** 3'-**GGGAGGGAATCA**	71.5	49	52.2
S15-0A	5'-**TTCACTAAGGGAGGG**-3'	-	88.1	90.6
H3A	5'-CGCTGGCTTT**TT** ||||||||| **C** 3'-**G**c**GAG**c**GAA**a**CA**	74.5	0	0
S15-3A	5'-**TTCAC**a**AAG**c**GAG**c**G**-3'	-	0	0
H4A	5'-CCCTCCCTTAaa ||||||||| a 3'-**GGGAGGGAAT**a**A**	69	29.6	31.3
S15-4A	5'-aaa**A**a**TAAGGGAGGG**-3'	-	35	38
H4B	5'-GGCTGGCTTA**TT** ||||||||| **C** 3'-cc**GA**cc**GAATCA**	76	0	0
S15-4B	5'-**TTCACTAAG**cc**AG**cc-3'	-	48.6	50
S15-5	5'-**TTCACTA**ttc**G**t**G**c**G**-3'	-	0	0
Duplex DNA (DD)	5'-**TAAGGGAGGG**-3' |||||||||| 3'-*ATTCCCTCCC*-5'	46	28.9	41.9
S10-0B	5'-**TAAGGGAGGG**-3'	-	34.1	38.4
C10-0A	5'-CCCTCCCTTA-3'	-	5	5
Partial Duplex (PD)	5'-aaa**A**a**TAAGGGAGGG**-3' |||||||||| 3'-*ATTCCCTCCC*-5'	46	32.2	38

[a] Bases in the ODNs complementary to RNA target are in boldface type. Base changes in the target complementary segment within an ODN are shown as lower case letters. The nontarget complementary strand sequence in the hairpin, duplex, and partial duplex DNA is shown in italicized letters.

hybrid under RNase H buffer conditions. Nonetheless, RNase H was able to cleave the RNA in the presence of this hairpin DNA as well as other hairpin and duplex DNAs that contained a complementary sequence at least 10 nt long. The results indicate that a stable base paired strand can serve as a template for RNase H cleavage of a RNA site. These findings present a new perspective of this enzyme's activity that may be pertinent to understanding its in vivo behavior, and in the development of new antisense therapeutics.

MATERIALS AND METHODS

Oligodeoxynucleotides. Oligodeoxynucleotides were obtained from Operon Technologies, Inc., Alameda, CA, or from the Emory University Microchemical Facility, Atlanta, GA, and purified by reverse-phase HPLC. The sequence of the ODNs is described in Table 1. ODN concentrations were estimated from absorbance values at 260 nm (37). The 5' termini of some oligomers were radioactively labeled with ^{32}P using T4 polynucleotide kinase. Ten picomoles of oligomer was incubated with 5.0 μL of [^{32}P]ATP (sp act. 6000 Ci/mmol; 10 mCi/mL), 6 units of T4 polynucleotide kinase in buffer containing 50 mM Tris-HCl (pH 7.6), 10

mM MgCl$_2$, 5 mM dithiothreitol, 0.1 mM spermidine hydrochloride, and 0.1 mM Na$_2$EDTA (pH 8.0). The reaction was incubated for 45 min at 37 °C, and then stopped by heating the sample at 68 °C for 10 min. The labeled ODNs were purified using the Nucleotide Removal Kit (QIAGEN Inc.).

Plasmid Used for Transcription. The pGEM7Zf(+) plasmid from Promega Inc. was modified to provide a template for RNA transcription. A 30 nt sequence from the HIV-1 reverse transcriptase gene containing 10 consecutive pyrimidines was inserted into the plasmid multiple cloning site. We refer to this new plasmid as pN1 (K. H. Nam, unpublished). Two partially complementary DNA oligomers (5'-GCGCGGGCCCGTTGTCAATACCCCTCCCTT-3' and 5'-GTCGGAATTCTAATTTCACTAAGGGAGGGG-3') were hybridized and filled in by Taq DNA polymerase. The underlined bases are from HIV-1. After digestion with *Apa*I and *Eco*RI, the duplex oligomer was ligated into pGEM7Zf-(+) between the *Apa*I and *Eco*RI restriction sites downstream of a T7 promoter. The plasmid was treated with calf intestinal alkaline phosphatase prior to ligation. The ligated plasmid was transformed into *E. coli* JM109 cells, and colonies were selected for ampicillin resistance. The desired construct was identified by *Dde*I digestion. pN1 generates five fragments, while the parent plasmid produces four *Dde*I bands.

In Vitro Transcription Reaction and RNA Purification. RNA transcripts were produced using *Hin*dIII-cut pN1 plasmid as the template for T7 RNA polymerase. A 1 mL transcription reaction contained 10 mM dithiothreitol, 500 μM each of ATP, CTP, GTP, and UTP, 1× transcription buffer (50 mM Tris-HCl, pH 7.5, 10 mM NaCl$_2$, 6 mM MgCl$_2$, and 2 mM spermidine), 25 units of Prime RNA inhibitor (5 Prime→3 Prime, Inc.), 0.1 mg of BSA (1 mg/mL), 120 units of T7 RNA polymerase, and 100 μg of the *Hin*dIII-digested pN1 plasmid DNA. Transcription reactions were carried out in a 37 °C water bath for 3 h. Afterward, the pN1 plasmid template was separated from the remaining reaction components with a Centricon-100 concentrator (Amicon). The filtrate was collected and transferred to a Centricon-10 concentrator and centrifuged at 1000g to concentrate the RNA and to remove smaller molecules. The last step was repeated several times. RNA concentration was estimated from its molecular weight and UV absorbance at 260 nm. It was assumed that 1.0 OD at 25 °C equals 40 μg/mL (*38*). RNA was also characterized by PAGE (Figure 1).

Melting Curve Characterization of DNAs. UV absorbance was employed to monitor the melting transition of the hairpin and duplex oligodeoxynucleotides at 268 nm with a DMS 300 spectrophotometer (Varian Inc.). Samples were heated at a rate of 0.4 °C/min using a circulating water bath. Temperature was measured with a platinum resistant probe inserted in a solvent cell adjacent to the sample. Absorbance and temperature signals were digitized and collected at 30 s time intervals. A temperature range from 15 to 95 °C was used. The buffer employed for the transition studies was either 100 mM NaCl, 10 mM sodium phosphate (pH 7.4), and 0.5 mM Na$_2$EDTA, or the 1× RNase H buffer [20 mM KCl, 10 mM MgCl$_2$, 20 mM Tris-HCl (pH 7.5), and 0.1 mM Na$_2$EDTA].
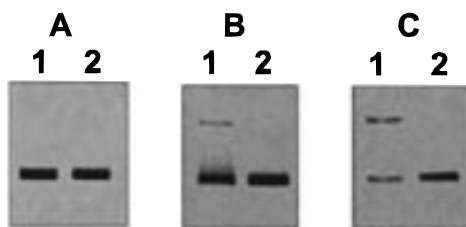
FIGURE 1: 79 nt RNA band pattern in denaturing and nondenaturing gels. (A) 12% gel with 8 M urea in TBE buffer. Lane 1: 15 pmol of RNA incubated at 65 °C for 3 min. Lane 2: RNA heated at 90 °C for 3 min. (B) 12% gel with TBE buffer. Lane 1: RNA without preheating. Lane 2: RNA preheated at 90 °C for 3 min. (C) 12% gel with TBE buffer and 5 mM Mg²⁺. Lane 1: RNA without preheating. Lane 2: RNA preheated at 90 °C for 3 min and quickly cooled.

Predicting the Relative Stability of RNA/DNA, RNA/RNA, and DNA/DNA Structures. To estimate the amount of hybrid formed between a DNA oligomer and its target site in a RNA, a thermodynamic analysis was made based on the free energies of formation for RNA/DNA, RNA, and DNA secondary structures. The analysis employed published thermodynamic parameters for a 1 M Na⁺ solvent (*31, 39, 40*) and the nearest-neighbor model (*40*) of nucleic acid stability. The free energy difference between two RNA secondary structures was estimated using the MFOLD algorithm, version 2.23 (*41, 42*). The free energy of a RNA/DNA duplex relative to its constituent single strands includes stacking interaction terms and a helix initiation factor. Thus, for the example of r(CCCUCCCUUA)/d(GGGAGGGAAT), the predicted free energy for forming this duplex at 25 °C is

$$\Delta G°_{25}(\text{R/D}) = \Delta G°_{25}(\text{rCC/dGG}) + \Delta G°_{25}(\text{rCC/dGG}) +$$
$$\Delta G°_{25}(\text{rCU/dAG}) + \Delta G°_{25}(\text{rUC/dGA})$$

$$+ \Delta G°_{25}(\text{rCC/dGG}) + \Delta G°_{25}(\text{rCC/dGG}) +$$
$$\Delta G°_{25}(\text{rCU/dAG})$$

$$+ \Delta G°_{25}(\text{rUU/dAA}) + \Delta G°_{25}(\text{rUA/dTA}) +$$
$$3.1 \text{ kcal/mol}$$

The last term is the helix initiation factor.

The free energy change at 25 °C of forming a hairpin DNA from its single-stranded form was calculated using the formula: $\Delta G°_{25} = \Delta G°_{25S} + \Delta G°_L(n)$. $\Delta G°_{25S}$ is the free energy of the hairpin stem, and $\Delta G°_L(n)$ is the free energy of the hairpin loop with n bases (*40*). $\Delta G°_L(n)$ is the sum of the free energy for initiating a loop of size L, and the stacking free energy of the base pair closing the loop and the adjacent mismatched bases of the loop. Parameters for DNA hairpin loops were obtained from J. SantaLucia (Web page, personal communication). $\Delta G°_{25S}$ was calculated using stacking parameters for a DNA duplex extrapolated to 25 °C (*39*).

One hairpin DNA, H0A, contained adjacent G·A mismatches and a G·G mismatch in the stem (Table 1). Nearest-neighbor stacking energies involving these mismatches were estimated from the literature. Li and Agrawal (*43*) evaluated thermodynamic parameters for melting a 6 bp duplex DNA with the same (CGAC)·(GGAG) sequence used in H0A, and two other DNAs with related Watson−Crick base pair sequences. Using the free energies of these molecules and

the known base pair stacking energies yielded a value of −4.7 kcal/mol for the sum of the three stacking free energies encompassing the two GA mismatches at 25 °C. The free energy for the G·G mismatch in (CGT)·(AGG) was estimated from an analogous sequence examined by Aboul-ela et al. (*44*). Their study evaluated thermodynamic parameters from the melting curve of a 9 bp DNA containing the sequence (TGT)·(AGA). By comparing the free energy of this DNA with homologous Watson−Crick base paired DNAs, a value of +0.4 kcal/mol was estimated for the two stacking terms containing the G·G mismatch.

Gel Mobility Shift Assay. RNA was added to³²P-labeled oligomer in a 1× TBE buffer (89 mM Tris−borate + 1 mM EDTA) containing 5 mM MgCl₂. Zero to fifteen picomoles of RNA was mixed with 0.5 pmol of DNA in10 μL volumes. After incubating at 25 °C for 30 min, samples were mixed with 2 μL loading buffer (30% Ficol and bromophenol blue) and loaded onto a 10% native polyacrylamide gel. The gel buffer was TBE and 5 mM MgCl₂, pH 8.0−8.3. The gel was run at room temperature at 100 V using a BRL vertical gel system. After electrophoresis, the gel was dried for 1 h and then scanned using the AMBIS radioisotope imaging system.

RNase H Assays. A 'master mixture' (60 μL) containing the RNA and *E. coli* RNase H1 (USB) was preincubated for 15 min at 25 °C in RNase H buffer with 0.15 unit of prime RNase inhibitor; 7 μL from this mixture was added to each reaction tube with 3 μL of a given DNA. Each reaction was incubated at 25 or 37 °C for 15 or 30 min. Samples were heated at 90 °C for 2−3 min and then quickly put on ice. They were mixed with ficol loading buffer, and run immediately into a 12% native PAGE. In some experiments, reactions were stopped by mixing the samples directly with the loading buffer and immediately run into the gel. The heating−cooling step produced a more rapid quenching of the reaction, but did not otherwise affect the results. In most experiments, 0.5 unit of RNase H was used per reaction, and the RNA and DNA concentrations were 1.5 and 9 μM, respectively. Nucleic acid bands were visualized by staining the gel with ethidium bromide solution followed by UV-induced fluorescence. Gel images were captured with a video gel documentation system. Exposure times were adjusted to produce images of the uncut RNA band in a linear intensity range. The relative intensities of the RNA bands were determined using the NIH Gel Image Analysis program, version 1.67. Percentage degradation values were reproducible within ±5%.

RESULTS

Characteristics of DNA and RNA Molecules. The five DNAs, H0A, H0B, H3A, H4A, and H4B, are each 25 nt long and can form hairpin structures with 10 bp stems and 5 base loops (Table 1). H0A and H0B share the same target binding sequence in their five base loop and the 3′ side of their stems. This stretch of nucleotides is complementary to a 15 nt long target within the 79 nt RNA sequence (Figure 2). H0A and H0B differ in stability due to differences in their stems. H0A has three mismatches in the stem, whereas H0B has all Watson−Crick base pairs. The other three hairpin DNAs, H3A, H4A, and H4B, shown in Table 1 differ from H0B by three or four base pair transversions or base
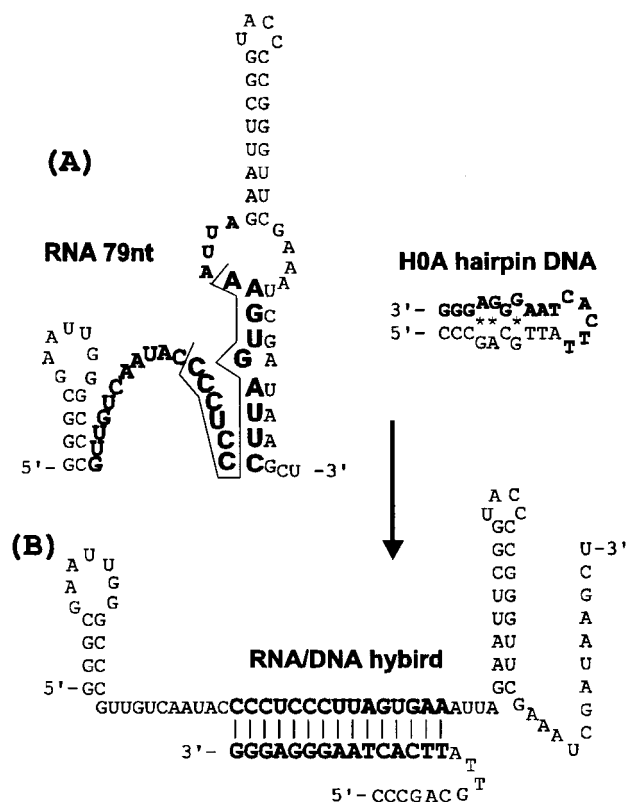
FIGURE 2: (A) Most stable secondary structure predicted for the 79 nt RNA by Zuker's algorithm. The targeted sequence is highlighted. (B) Schematic of RNA/DNA formation with hairpin DNA, H0A.

FIGURE 3: Normalized UV absorbance−melting curves of the four hairpin DNAs listed and the 10 bp duplex, DD, in the RNase H assay buffer.

substitutions in the stem or loop portion of the target binding sequence. The single-stranded DNAs, S15-0A, S15-3A, S15-4A, and S15-4B, correspond to the 15 nt long target binding segment of the hairpin DNAs H0A, H3A, H4A, and H4B, respectively. Two duplex DNAs were employed; a 10 bp duplex (DD) formed with the single strands S10-0B and C10-0A, and a 10 bp duplex with a 5 nucleotide dangling end formed with strands C10-0A and S15−4A.

The 79 nt RNA was characterized by its electrophoretic mobility under different conditions. When it was preheated to 90 °C for 2−3 min and quickly cooled, the RNA produced only one band in a 12% denaturing polyacrylamide gel (Figure 1A). If the RNA was not preheated prior to loading, two bands were observed in a 12% nondenaturing polyacrylamide gel with TBE as the gel buffer (Figure 1B). The faster moving band was dominant. When the RNA was run in a 12% polyacrylamide gel using the Tris−borate buffer with 5 mM MgCl₂ replacing the Na₂EDTA, the two bands had essentially equal intensity (Figure 1C). These results indicate that one major RNA species was transcribed, but that it can form two conformations or monomer and dimer with distinct gel mobilities. The relative amount of each species was dependent on the sample's temperature history and solvent. Figure 2A shows the lowest energy RNA secondary structure predicted by Zuker's MFOLD algorithm version 2.23 (*41, 42*). The predicted structure indicates that part of the target sequence is single stranded while the other part forms a duplex segment. A similar situation occurs with the four similar secondary structures that are within a kilocalorie of the minimum energy structure.

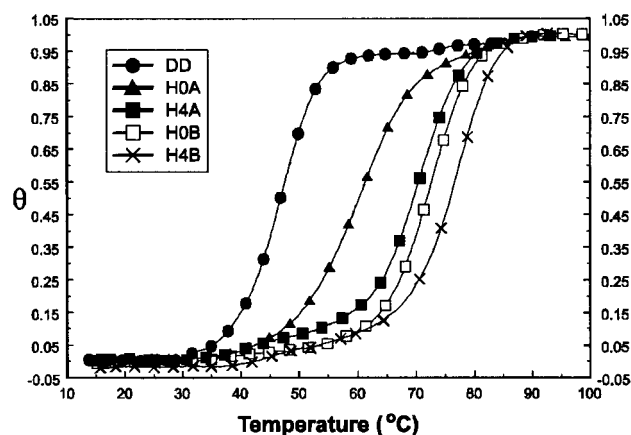Figure 3 shows the denaturation transitions of four hairpin

DNAs and one duplex DNA in the RNase H buffer. T_m values are listed in Table 1. The hairpin DNA transitions are single-step curves with T_m values consistent with similar hairpin DNA structures (*45*). The transitions were reversible and independent of a 15-fold change in DNA concentration. Melting transitions were also obtained in 0.1 M NaCl (not shown). They gave similar profiles and T_m values. Single-stranded oligonucleotides did not exhibit melting transitions, indicating the absence of self-structures. No significant difference was observed between the transition of the duplex DD formed by S10-0B and C10-0A, and the partial duplex with the five base tail PD (not shown).

Predicting Equilibrium Hybridization of DNA to RNA. The probability that a DNA oligomer binds to a complementary target site within a folded RNA molecule depends on the stability of the RNA/DNA hybrid vs competing DNA and RNA self-structures. Kinetic factors may also influence binding. As a first step toward assessing the interaction of the DNAs in this study with the target site in the 79 nt RNA, the equilibrium binding of a DNA oligomer to the RNA target was analyzed. Although two RNA conformers are indicated under the reaction conditions, we assume both present the target structure in a similar way, and treat them as one molecule. The gel assay data are consistent with this assumption. The reaction between a hairpin DNA and a native RNA (R_n) to form a RNA/DNA hybrid can be written as

$$D_h + R_n \rightleftarrows R_o{\cdot}D_s, \quad \Delta G°_T \tag{1}$$

The standard state free energy change, $\Delta G°_T$, for eq 1 can be related to the free energy change of forming the $R_o{\cdot}D_s$ complex from an already 'open' RNA conformation (R_o) and the single-stranded form of the hairpin DNA (D_s):

$$R_o + D_s \rightleftarrows R_o{\cdot}D_s, \quad \Delta G°_1 \tag{2}$$

and the free energy changes of forming the hairpin DNA from the single-strand D_s, and of forming R_n from R_o:

$$D_s \rightleftarrows D_h, \quad \Delta G°_2 \tag{3a}$$

$$R_o \rightleftarrows R_n, \quad \Delta G°_3 \tag{3b}$$

Relating the equilibrium constants of reactions 1 to 3 yields

$$\Delta G^{\circ}_{T} = \Delta G^{\circ}_{1} - (\Delta G^{\circ}_{2} + \Delta G^{\circ}_{3}) \qquad (4)$$

ΔG°_{3} was calculated using the Zuker algorithm by assuming R_{n} to be the predicted lowest free energy structure for the 79 nt RNA, and R_{o} to be the lowest free energy structure with the 15 nt target sequence constrained to be single stranded. Formation of a RNA/DNA hybrid described by eq 1 will produce an unpaired tail at the 5' end of the hairpin DNA.

Using eq 4, and the thermodynamic parameters and assumptions described under Materials and Methods, the predicted ΔG°_{T} at 25 °C for the interaction of H0B with the RNA was −4.0 kcal/mol. This value was determined from calculations that yielded $\Delta G^{\circ}_{1} = -20.1$ kcal/mol for the 15 bp RNA/DNA hybrid, $\Delta G^{\circ}_{2} = -12.3$ kcal/mol for the hairpin DNA, and $\Delta G^{\circ}_{3} = -3.8$ kcal/mol for the RNA conformational change. For the hairpin DNA H0A, $\Delta G^{\circ}_{T} = -8.0$ kcal/mol based on a ΔG°_{2} value of −8.3 kcal/mol. The free energy change for binding other hairpin DNAs to the RNA were determined in a similar way. They depend on the hairpin stability (ΔG°_{2}), and the number of base pairs in the RNA/DNA hybrid (ΔG°_{1}). The free energy for binding a single-stranded DNA to the RNA, for example, S15-0A, was determined by ignoring ΔG°_{2} in eq 4. The value of ΔG°_{T} for S15-0A was −16.3 kcal/mol.

Since the above calculations assume a solvent of 1 M Na$^+$, it is uncertain if they are appropriate for predicting RNA/DNA formation under the experimental conditions used. Arguments justifying the application of 1 M Na$^+$ parameters to solvents similar to ours (i.e., containing 5−10 mM Mg^{2+}) have been made by Yager and Von Hippel (*46*). Although exact agreement with experiment is not expected, the equilibrium calculations should provide an estimate of the *relative* amounts of RNA/DNA hybrid occurring for the different DNAs.

Gel Mobility Shift Assay of DNA/RNA Hybridization. The interaction of the 79 nt RNA molecule with the hairpin DNAs H0A and H0B and the single-stranded DNA S15-0A was examined using a mobility shift assay. The ^{32}P-labeled DNAs were mixed with varying amounts of unlabeled 79 nt RNA and incubated for 30 min at 25 °C prior to electrophoresis in a 10% polyacrylamide gel. Titration of 0.05 µM of the hairpin DNA H0B with up to a 30-fold higher amount of the RNA yielded only the free DNA band (not shown). Figure 4A shows a similar gel shift experiment using ^{32}P-labeled H0A and the RNA. A small amount of H0A is observed in two shifted bands when the ratio of RNA to H0A was above 10:1. These bands correspond to complexes formed with the RNA species observed in the Mg^{2+} polyacrylamide gel (Figure 1C). The equal intensities of the shifted bands imply that H0A binds equally to both RNA conformers. The total percentage of H0A hybridized to the RNA was 6%, 8%, and 9% for molar ratios of RNA:DNA of 10:1, 15:1, and 30:1, respectively. The binding of S15-0A to the RNA was more substantial (Figure 4B). The percentage of S15-0A bound was 11%, 38%, 55%, and 63% when the RNA:DNA molar ratio was 2:1, 10:1, 15:1, and 30:1, respectively. The inability of saturating levels of RNA to bind all S15-0A may be due to kinetic factors relating to the slow dissociation rate of RNA self-structures.

The above results were compared to predictions based on the calculated free energy changes for the three DNA−RNA
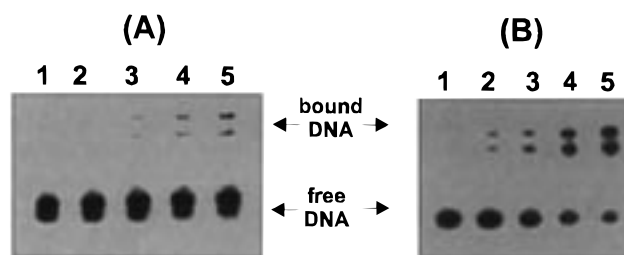

FIGURE 4: 10% PAGE mobility shift assay. In both panel A and panel B, lanes 1−5 containing 0, 1, 5, 10, and 15 pmol of the 79 nt RNA, respectively, were mixed with (A) 0.5 pmol of ^{32}P-labeled single-strand S15-0A or (B) 0.5 pmol of the H0A hairpin DNA.

Table 2: Calculated ΔG° Values for RNA/DNA Hybrid Formation at 25 °C, and Predicted Fraction of DNA Hybridized to RNA Assuming 1.5 µM RNA and a 30:1 RNA to DNA Ratio[a]

DNA	ΔG°_{1} (kcal/mol)	ΔG°_{2} (kcal/mol)	ΔG°_{3} (kcal/mol)	$\Delta G_{25}^{\circ}{}_{T}$ (kcal/mol)	predicted fraction bound
H0A	−20.1	−8.3	−3.8	−8.0	0.5
H0B	−20.1	−12.3	−3.8	−4.0	~10^{-3}
S15-0A	−20.1	0	−3.8	−16.3	1.0
H4A	−12.0	−12.2	−1.4	1.6	0
S15-4A	−12.0	0	−1.4	−10.6	1.0
DD	−12.0	−13.6	−1.4	3.0	0
PD	−12.0	−13.6	−1.4	3.0	0
S10-0B	−12.0	0	−1.4	−10.6	1.0

[a] ΔG°_{1}, ΔG°_{2}, ΔG°_{3}, and ΔG°_{T} are defined by eqs 1−4. ΔG°_{2} is also used here to represent the free energy of forming a duplex DNA from single strands.

interactions, and the concentrations employed. For the binding of H0B to RNA, ΔG°_{T} is −4.0 kcal/mol, and the fraction of DNA hybridized to RNA is predicted to be negligible (~10^{-3}) at the 30:1 RNA to DNA ratio. This is consistent with the experimental result. For the hairpin DNA H0A, the fraction of DNA hybridized to RNA is predicted to be 25% at the 10:1 RNA:DNA ratio, and 32% for a 15:1 ratio. These values are about 4-fold higher than the observed values. For S15-0A, the calculations predict 100% of the DNA is bound at a 2:1 ratio of RNA to DNA. This is again higher than the observed value of 11%. The calculations are in qualitative accord with the relative affinity of the three DNAs with the RNA, but predict higher amounts of RNA/DNA hybrid than was measured. This is consistent with the notion that slow dissociation rates of RNA and DNA self-structures inhibit intermolecular hybridization. Table 2 lists the free energy values used to determine ΔG°_{T} and the estimated fraction of DNA bound to RNA at a 30:1 RNA:DNA ratio.

RNase H Can Cleave a Target RNA in the Presence of a Stable Hairpin DNA. A RNase H assay was carried out to test for RNA digestion in the presence of the hairpin DNAs H0A and H0B as well as the other DNA oligomers. Figure 5A shows the results of incubating 0.5 unit of RNase H at 25 °C for 30 min with 1.5 µM RNA and 9 µM various DNAs. Lane 1 shows a control in which RNase H was incubated with RNA alone. A single band corresponding to the undigested RNA is observed. Lanes 2−4 show the results with the DNAs H0B, H0A, and S15-0A. The percentage of RNA degraded was 49%, 71%, and 88% for H0B, H0A, and S15-0A, respectively. The hairpin DNAs H0A and H0B have melting temperatures well above the reaction conditions in the RNase H buffer (Table 1).
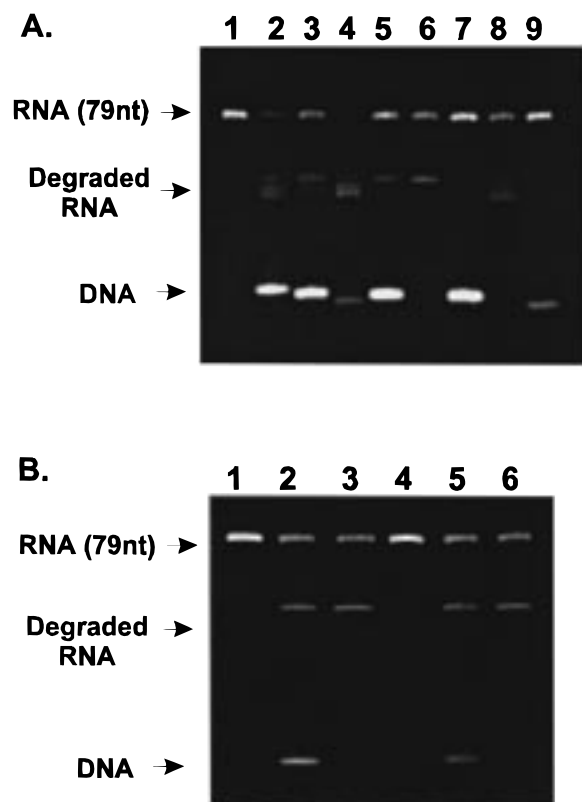
A.

B.

FIGURE 5: RNase H assay of RNA degradation. The 79 nt RNA (15 pmol) was incubated with 90 pmol of DNA and 0.5 unit of RNase H at 25 °C for 30 min. Reactions were stopped and run on a 12% native gel. Lane 1 in both panel A and panel B contained RNA alone. (A) Lanes 2–9: RNA with H0A, H0B, S15-0A, H4A, S15-4A, H4B, S15-4B, and S15-5A, respectively. (B) Lanes 2–6: RNA with DD, S10-0B, C0, PD, and S15-4A, respectively.

The effect of changing the hairpin loop sequence of H0B on RNase H cleavage was examined. Four of the five loop nucleotides in H0B were changed such that they are no longer complementary to the RNA target. This molecule is referred to as H4A. The 3′ strand of the H4A stem has 10 consecutive complementary bases to the RNA target. The T_m of the DNA is 69.5 °C. Lane 5 of Figure 5A shows that this hairpin DNA serves as a template to degrade ~30% of the RNA, but with RNA fragments different from H0B or H0A. This cleavage pattern was also observed when the single strand S15-4A was used as a template (lane 6, Figure 5A). The latter DNA has the same 10 complementary bases as H4A (Table 1) and results in 35% RNA degradation.

For the concentrations employed, equilibrium calculations using the standard state free energies estimated earlier predict that 100% of the RNA forms a RNA/DNA hybrid with S15-0A, 80% of the RNA is hybridized by H0A, but essentially no RNA forms a hybrid with H0B (~0.7%) or H4A (0%). The degradation of 49% of the RNA with H0B or 30% with H4A is thus unexpected, particularly since the predicted amounts of hybrid are likely to be upper limits.

No detectable RNA degradation was found with the single-stranded DNAs S15-5 and S15-3A, which have five and three base changes interspersed in the15 nt sequence, or with hairpin DNAs H3A and H4B. The latter two DNAs differ from H0B by three or four base pair transversions in the stem. Although H4B has a nine base segment that is complementary to the target RNA, this was insufficient to

overcome the inhibitory effect of the hairpin stability. The single strand S15-4B, which has the same complementary sequence as H4B, induces 48% degradation of the RNA.

The RNase H assay was also conducted with the same molecules and concentrations at 37 °C. The results were similar to that shown at 25 °C (not shown). The percentage of RNA degraded at this temperature was 52%, 79%, and 91% for the DNAs H0B, H0A, and S15-0A, respectively. H4A produced 31% RNA degradation. As observed at 25 °C, no degradation of the RNA occurred with hairpin DNAs H3A or H4B, or with single strands S15-3A or S15-5. Degradation of the RNA with H0A, H0B, and H4A was also observed at a lower DNA:RNA ratio of 3 μM DNA to 1.5 μM RNA at 37 °C (not shown). The percentage of RNA degraded was 55%, 51%, and 21%, respectively. No significant RNA degradation was seen with H4B or S15-5 at 10-fold higher amounts of RNase H.

The results of the RNase H assay with duplex DNA, duplex DNA with a dangling end, and corresponding single-stranded DNAs are shown in Figure 5B and listed in Table 1. RNA degradation occurred with the duplex DD, and the partial duplex PD. These DNAs present the same complementary 10 base sequence as S10-0B and S15-4A, and they produced a similar digestion pattern. The percentage of RNA degradation at 25 °C was about 30% for both the duplexes as well as the single strands (Table 1). At 37 °C, the percentage of RNA degraded was approximately 40%. An estimate of the RNA/DNA hybrid concentration expected from the initial concentrations of DD (or PD) and the RNA was made using an equilibrium analysis similar to that given in eqs 1–4. The length of the hybrid was 10 bp, and eq 3a describes the duplex to strand dissociation. $\Delta G°_T$ for this reaction was calculated to be +3.2 kcal/mol, and the fraction of RNA/DNA hybrid was zero. Yet, as with the cases of H0B and H4A, RNase H digestion occurs with DD or PD duplexes, even though equilibrium analysis does not predict hybrid formation.

DISCUSSION

The results show that a base paired strand of a hairpin DNA can serve as a template for RNase H cleavage of a target RNA at a temperature well below the T_m of the DNA. The extent of degradation was sensitive to the length and location of the complementary target binding segment in the hairpin DNA. Altering four complementary bases in the hairpin loop of H0B to give H4A reduced RNA degradation 1.6-fold, but did not eliminate it. Thus, a complementary loop sequence in a hairpin DNA is not absolutely required for the formation and cleavage of the RNA/DNA hybrid. Changing three or four base pairs in the stem of H0B to produce H3A and H4B, respectively, completely eliminated RNA cleavage by RNase H. Both target complementary and hairpin DNA stability appear to be important factors in these outcomes.

The need for a minimum stretch of complementary bases, independent of the DNA structure, is indicated by the results with S15-3A and S15-5. S15-3A has the same target binding region as H3A; a 5 base stretch and two 3 base stretches interrupted by single mismatches. Although single stranded, S15-3A is unable to template RNA degradation. S15-5, which has 7 contiguous complementary bases, is also unable

to template RNA degradation. However, the single strand S15-4B, which has the same 9 base target binding segment as hairpin H4B, does serve as a template for RNA degradation. The latter result suggests that the hairpin's stability inhibits the reaction. A comparison of RNase H activity in the presence of H0A vs H0B supports this conclusion. H0A and H0B have the same 15 nt target binding sequence, but differ in stability. H0A has the lower stability and produced about 1.5 times more degradation in the RNase H assay.

Two hypotheses can explain the ability of RNase H to degrade the 79 nt RNA at temperatures below the T_m of hairpin and duplex DNA templates. The first hypothesis assumes that the exchange of base pairing from within a hairpin or duplex DNA to a RNA target site is thermodynamically favorable under RNase H reaction conditions. The second hypothesis supposes that RNase H can promote formation and cleavage of a RNA/DNA complex even if the equilibrium reaction of the RNA and DNA alone does not favor hybrid formation. The thermodynamic calculations and experimental studies of hybrid formation favor the second hypothesis.

The equilibrium predictions of RNA/DNA hybrid formation were in qualitative but not quantitative agreement with the results from the gel shift experiments. In all cases that could be measured, the predicted amount of hybrid was higher than the observed values. While this could be due to experimental artifacts, it is consistent with the existence of activation barriers between RNA and DNA self-structures and the intermolecular hybrid. Kinetic barriers to intermolecular hybridization have been described for complementary RNA hairpins (*47*). Assuming the predicted amounts of RNA/DNA complexes are upper limits, the observed degradation of the 79 nt RNA with H0B, H4A, DD, or PD as templates is completely unanticipated. Essentially no RNA/DNA hybrid is predicted to form with these DNAs. This implies that RNase H helps to stabilize the formation of a RNA/DNA hybrid from a RNA target and a complementary strand within a hairpin or duplex DNA.

Studies using oligodeoxynucleotides (ODNs) as antisense molecules have indicated that cellular RNase H activity is an important element in the antisense effect (*25, 26*). An ODN is thought to inhibit a given gene's expression by hybridizing to a specific mRNA and providing a target for RNase H. If this is an accurate view, our results suggest that stable DNA hairpin molecules can provide a new approach for enhancing antisense specificity. By modulating the stability of the hairpin DNA without changing its target binding segment, it should be possible to enhance the specificity of RNase H cleavage for the completely complementary sequence vs partially complementary sequences. The efficacy of this type of 'stringency clamp' effect (*48*) will depend on both thermodynamic aspects of the RNA−DNA interaction and kinetic considerations of intermolecular hybridization and RNase H cleavage rates. The hairpin structure will also enhance the lifetime of the antisense molecule since it is resistant to nuclease digestion (*49*).

ACKNOWLEDGMENT

REFERENCES

1. Cote, J., and Ruiz-Carrillo, A. (1993) *Science 261*, 765−769.
2. Baker, T. A., and Kornberg, A. (1988) *Cell 55*, 113−123.
3. Kowalski, J., and Denhardt, D. T. (1979) *Nature 281*, 704−706.
4. Turchi, J. J., Huang, L., Murante, R. S., Kim, Y., and Bambara, R. A. (1994) *Proc. Natl. Acad. Sci. U.S.A. 91*, 9803−9807.
5. Okazaki, R., Sugimoto, K., Okazaki, T., Imae, Y., and Sugino, A. (1970) *Nature 228*, 223−226.
6. von Hippel, P. H., and Yager, T. D. (1992) *Science 255*, 809−812.
7. Varmus, H. (1988) *Science 240*, 1427−1435.
8. Daniels, G. A., and Lieber, M. R. (1995) *Nucleic Acid Res. 23*, 5006−5011.
9. Reaban, M. E., and Griffin, J. A. (1990) *Nature 348*, 342−344.
10. Feng, J. L., Funk, W. D., Wang, S. S., Weinrich, S. L., Avilion, A. A., Chiu, C. P., Adams, R. R., Chang, E., Allsopp, R. C., Yu, J. H., Le, S. Y., West, M. D., Harley, C. B., Crews, W. H., Greider, C. W., and Villeponteau, B. (1995) *Science 269*, 1236−1241.
11. Blasco, M. A., Funk, W., Villeponteau, B., and Greider, C. W. (1995) *Science 269*, 1267−1270.
12. Matteucci, M. D., and Wagner, R. W. (1996) *Nature 384*, 20−22.
13. Rong, Y. W., and Carl, P. L. (1990) *Biochemistry 29*, 383−389.
14. Campbell, A. G., and Ray, D. S. (1993) *Proc. Natl. Acad. Sci. U.S.A. 90*, 9350−9354.
15. Eder, P. S., Walder, R. Y., and Walder, J. A. (1993) *Biochimie 75*, 123−126.
16. Itaya, M., and Kondo, K. (1991) *Nucleic Acids Res. 19*, 4443−4449.
17. Mueser, T C., Nossal, N. G., and Hyde, C. C. (1996) *Cell 85*, 1101−1112.
18. Wei, X., and Peterson, D. L. (1996) *J. Biol. Chem. 271*, 32617−32622.
19. Peliska, J. A., and Benkovic, S. J. (1992) *Science 258*, 1112−1118.
20. Crooke, S. T., Lemonidis, K. M., Neilson, L., Griffey, R., Lesnik, E. A., and Monia, B. P. (1995) *Biochem. J. 312*, 599−608.
21. Uchiyama, Y., Miura, Y., Inoue, H., Ohtsuka, E., Ueno, Y., Ikehara, M., and Iwai, S. (1994) *J. Mol. Biol. 243*, 782−791.
22. Katayanagi, K., Miyagawa, M., Matsushima, M., Ishikawa, M., Kanaya, S., Ikehara, M., Matsuzaki, T., and Morikawa, K. (1990) *Nature 347*, 306−309.
23. Ogawa, T., and Okazaki, T. (1984) *Mol. Gen. Genet. 193*, 231−237.
24. Rumbaugh, J. A., Murante, R. S., Shi, S., and Bambara, R. A. (1997) *J. Biol. Chem. 272*, 22591−22599.
25. Boiziau, C., Moreau, S., and Toulme, J. J. (1994) *FEBS Lett. 340*, 236−240.
26. Monia, B. P., Lesnik, E. A., Gonzalez, C., Lima, W. F., McGee, D., Guinosso, C. J., Kawasaki, A. M., Cook, P. D., and Freier, S. M. (1993) *J. Biol. Chem. 268*, 14514−14522.
27. Donis-Keller, H. (1979) *Nucleic Acids Res. 7*, 179−192.
28. Serra, M. J., Barnes, T. W., Betschart, K., Gutierrez, M. J., Sprouse, K. J., Riley, C. K., Stewart, L., and Temel, R. E. (1997) *Biochemistry 36*, 4844−4851.
29. SantaLucia, J., Jr., Allawi, H. T., and Seneviratne, P. A. (1996) *Biochemistry 35*, 3555−3562.
30. Sugimoto, N., Nakano, S., Yoneyama, M., and Honda, K. (1996) *Nucleic Acids Res. 24*, 4501−4505.
31. Sugimoto, N., Nakano, S., Katoh, M., Matsumura, A., Nakamuta, H., Ohmichi, T., Yoneyama, M., and Sasaki, M. (1995) *Biochemistry 34*, 11211−11216.
32. Lesnik, E., and Freier, S. M. (1995) *Biochemistry 34*, 10807−10815.
33. Roberts, R. W., and Crothers, D. M. (1992) *Science 258*, 1463−1466.
34. Riley, M., Maling, B., and Chamberlin, M. J. (1966) *J. Mol. Biol. 20*, 359−389.

35. Martin, F. H., and Tinoco, I., Jr. (1980) *Nucleic Acids Res. 8,* 2295−2299.
36. Gurgo, C., Guo, H.-G., Franchini, G., Aldovini, A., Collalti, E., Farrell, K., Wong-Staal, F., Gallo, R. C., and Reitz, M. S., Jr. (1988) *Virology 164,* 531−536.
37. Lautenberger, J. A. (1991) *BioTechniques 10,* 778−780.
38. Sambrook, J., Fritsch, E. F., and Maniatis, T. (1989) *Molecular Cloning: A Laboratory Manual,* 2nd ed., Cold Spring Harbor Laboratory Press, Cold Spring Harbor, NY.
39. Allawi, H. T., and SantaLucia, J., Jr. (1997) *Biochemistry 36,* 10581−10594.
40. Serra, M. J., and Turner, D. H. (1995) *Methods Enzymol. 259,* 242−261.
41. Walter, A. E., Turner, D. H., Kim, J., Lyttle, M. H., Muller, P., Mathews, D. H., and Zuker, M. (1994) *Proc. Natl. Acad. Sci. U.S.A. 91,* 9218−9222.

42. Zuker, M. (1994) *Methods Mol. Biol. 25,* 267−294.
43. Li, Y., and Agrawal, S. (1995) *Biochemistry 34,* 10056−10062.
44. Aboul-ela, F., Koh, D., Tinoco, I., Jr., and Martin, F. H. (1985) *Nucleic Acids Res. 13,* 4811−4824.
45. Paner, T. M., Amaratunga, M., Doktycz, M. J., and Benight, A. S. (1990) *Biopolymers 29,* 1715−1734.
46. Yager, T. D., and von Hippel, P. H. (1991) *Biochemistry 30,* 1097−1118.
47. Eguchi, Y., and Tomizawa, J. (1991) *J. Mol. Biol. 220,* 831−842.
48. Roberts, R. W., and Crothers, D. M. (1991) *Proc. Natl. Acad. Sci. U.S.A. 88,* 9397−9401.
49. Tang, J. Y., Temsamani, J., and Agrawal, S. (1993) *Nucleic Acids Res. 21,* 2729−2735.